Reversible host cell surface remodelling limits immune recognition and maximizes transmission of *Plasmodium falciparum* gametocytes

Priscilla Ngotho[1,2], Kathleen Dantzler Press[3], Megan Peedell[1,2], William Muasya[1], Brian Roy Omondi[4], Stanley E. Otoboh[4], Karl B. Seydel[5,6], Melissa Kapulu[7], Miriam Laufer[8], Terrie Taylor[5,6], Teun Bousema[9], Matthias Marti[1,2*]

[1]Wellcome Centre for Integrative Parasitology, University of Glasgow, Glasgow, United Kingdom.

[2]Institute of Parasitology, Vetsuisse Faculty, University of Zurich, Zurich, Switzerland

[3]Department of Medicine, Stanford University School of Medicine, Stanford, CA, United States.

[4] Institute of Immunology and Infection Research, School of Biological Sciences, University of Edinburgh, Edinburgh, United Kingdom.

[5]Department of Osteopathic Medical Specialties, College of Osteopathic Medicine, Michigan State University, East Lansing, Michigan, United States.

[6]Blantyre Malaria Project, Kamuzu University of Health Sciences, Blantyre, Malawi

[7]KEMRI Wellcome Trust Research Programme, Kilifi, Kenya.

[8]Center for Vaccine Development and Global Health, University of Maryland School of Medicine Baltimore, MD, United States.

[9]Radboud Institute for Health Sciences, Radboud University Medical Center, Nijmegen, Netherlands.

*Correspondence to Matthias.Marti@glasgow.ac.uk

Abstract

Reducing malaria transmission has been a major pillar of control programmes and is considered crucial for achieving malaria elimination. Gametocytes, the transmissible forms of the *P. falciparum* parasite, arise during the blood stage of the parasite and develop through 5 morphologically distinct stages. Immature gametocytes (stage I-IV) sequester and develop in the extravascular niche of the bone marrow and possibly spleen. Only mature stage V gametocytes re-enter peripheral circulation to be taken up by mosquitoes for successful onward transmission. We have recently shown that immature, but not mature gametocytes are targets of host immune responses and identified putative target surface antigens. We hypothesize that these antigens play a role in gametocyte sequestration and contribute to acquired transmission-reducing immunity. Here we demonstrate that surface antigen expression, serum reactivity by human IgG, and opsonic phagocytosis by macrophages all show similar dynamics during gametocyte maturation, i.e., on in immature and off in mature gametocytes. Moreover, the switch in surface reactivity coincides with reversal in phosphatidylserine (PS) surface exposure, a marker for red blood cell age and clearance. PS is exposed on the surface of immature gametocytes (as well as in late asexual stages) but is removed from the surface in later gametocyte stages (IV-V). Using parasite reverse genetics and drug perturbations, we confirm that parasite protein export into the host cell and phospholipid scramblase activity are required for the observed surface modifications in asexual and sexual *P. falciparum* stages. These findings suggest that the dynamic surface remodelling allows (i) immature gametocyte sequestration in bone marrow and (ii) mature gametocyte release into peripheral circulation and immune evasion, therefore contributing to mature gametocyte survival *in vivo* and onward transmission to mosquitoes. Importantly, blocking scramblase activity during gametocyte maturation results in efficient clearance of mature gametocytes, revealing a potential path for transmission blocking interventions. Our studies have important implications for our understanding of parasite biology and form a starting point for novel intervention strategies to simultaneously reduce parasite burden and transmission.

Introduction

Plasmodium falciparum malaria remains a devastating global health burden despite concerted efforts towards control and elimination. Recent health service disruptions due to the COVID-19 pandemic resulted in a reversal of progress in reducing mortality and morbidity made in the last decade (WHO, 2021). The most effective approaches to curb malaria, vector control and prompt diagnosis and treatment, are challenged by insecticide and drug resistance. Their dependence on efficient health systems in economically and socio-political stable environments further highlights the need for additional approaches towards elimination in low-resource settings.

An essential component of malaria elimination is interrupting the transmission cycle from human to vector and back to human. Therefore, blocking transmission from human to vector is an attractive target for novel therapeutics. In the human host, *P. falciparum* cycles through various host cells and organs and extensively modifies these host cells for its metabolic needs for replication and transmission. During its blood stage cycle, *P falciparum* infects naïve red blood cells (RBCs) and replicates asexually every 48h hours, resulting in cyclic fevers to the host as well as other clinical manifestation of disease. A sub population of parasites differentiate to the sexual replicative forms (gametocytes) that are the only forms capable of transmitting to mosquitoes. Gametocytes primarily develop in hematopoietic niches of bone marrow and possibly spleen, a feature that is conserved across the *Plasmodium* lineage (De Niz *et al*, 2018; Joice *et al*, 2014; Kho *et al*, 2021a; Kho *et al*, 2021b; Lee *et al*, 2018; Obaldia *et al*, 2018) (Hentzschel *et al*, 2022). A unique feature of *P. falciparum* gametocytes is the prolonged development cycle that coincides with morphological differentiation delineating the 5 stages (I-V) of gametocytogenesis (Hawking *et al*, 1971). During this gametocyte maturation period, the host cell undergoes profound biophysical changes. Immature sequestering forms become rigid (Aingaran *et al*, 2012; Tiburcio *et al*, 2012a) and express antigens on the infected red blood cell (iRBC) surface (Dantzler *et al*, 2019). During maturation from stage IV to V, parasites switch into a deformable state without antigens on the iRBC surface. Hence, these deformable mature forms are immunologically silent, allowing release into circulation while avoiding both immune clearance and splenic filtration. Surface

antigens play a key role in sequestration of mature asexual parasites and are therefore hypothesized to mediate gametocyte sequestration as well. Immature gametocytes lack key features on the iRBC surface mediating asexual parasite sequestration, in particular knob structures and the major surface antigen and cytoadherence ligand PfEMP1 (Fraschka *et al*, 2018; Tiburcio *et al*, 2012b). Therefore, the mode of interaction with other cells in the hematopoietic niche remains unclear. We have previously identified potential surface antigens that may play this role, including GEXP07 and GEXP10 (Dantzler *et al.*, 2019; Hermand *et al*, 2016; Silvestrini *et al*, 2010). Importantly, once parasites are in circulation, surface exposed parasite antigens trigger immune clearance mechanisms such as opsonic phagocytosis (Dantzler *et al.*, 2019; Fraser *et al*, 2021a; Teo *et al*, 2015). Therefore, it would be in the parasites' interest to ensure these modifications only mark the iRBC surface while outside of circulation.

We hypothesise that temporary iRBC surface modifications during gametocyte development enable efficient sequestration of immature stages, while its reversal facilitates mature gametocyte exit from the hematopoietic niche and "safe" circulation in peripheral blood without detection and clearance by host immunity. Perturbation of this reversible process could prevent parasite sequestration or subsequent release into circulation, and/or expose immunogenic targets and reduce onward transmission of the parasite to the mosquito vector. Here, we have tested this hypothesis and demonstrate that reversible surface antigen exposure coincides with a reversible flipping of phosphatidylserine onto the iRBC surface, a process that can be blocked to trigger efficient phagocytosis of the otherwise immunologically "silent" mature gametocyte.

Results

Dynamics of surface antigen exposure in *P. falciparum* gametocytes

We recently carried out an analysis of surface antigen expression in *P. falciparum* gametocytes using a transgenic line (Pf2004 Tdtom) that expresses a fluorescent reporter starting at approximately 30 hours of gametocytogenesis (Aingaran *et al.*, 2012; Dantzler *et al.*, 2019). This study revealed that immune sera as well as specific antibodies raised against gametocyte surface antigens labelled the surface of immature

(Stage II/III) but not mature (Stage V) gametocyte-infected red blood cells (giRBC) (Dantzler *et al.*, 2019). To further define the dynamics of antigen expression, we carried out a time course during gametocyte maturation. For this purpose, we used both the Tdtom reporter line and a second reporter line that expresses a GFP-tagged version of the exported GEXP02 antigen (Portugaliza *et al*, 2019; Warncke *et al*, 2020). This antigen is expressed from early gametocyte development (i.e., gametocyte ring) and stays on throughout the sexual development cycle (Portugaliza *et al.*, 2019; Warncke *et al.*, 2020). Using a combination of flow cytometry and fluorescent microscopy, we measured giRBC surface recognition using a pool of highly reactive patient serum. We observed minimal surface recognition in gametocyte rings, followed by a gradual increase peaking at stage II gametocytes (**Figure 1A,B**). In asexual stages, a similar pattern was observed with minimal signal in ring stages and major recognition in schizonts (**Figure 1A,B**). After the peak at stage II, giRBCs lost surface antigen expression as they matured with minimal signal observed in stage V. We also measured surface reactivity against two iRBC surface antigens expressed both in asexual and gametocyte stages, PfGEXP07 and PfGEXP10 (Dantzler *et al.*, 2019; Hermand *et al.*, 2016) and observed that reactivity was limited to early developmental stages (**Figure 1C,D and S1**). The on and off pattern of giRBC immune recognition was in agreement with our previous observations (Dantzler *et al.*, 2019) and confirmed in the reference parasite line NF54 (**Figure S1**). Interestingly, permeabilization experiments revealed that most of the serum and GEXP10 signal remained within the iRBC and inside the parasite, even at peak recognition in stage II gametocytes. In contrast, only a small proportion is expressed on the iRBC surface (**Figure 1E-F and S2**). This is similar to observations in asexual stages, where only a fraction of the major surface protein, PfEMP1, is delivered to the iRBC surface while the majority remains within the host cell (Bengtsson *et al*, 2008). Quantification of antigen distribution based on immunoelectron microscopy using GEXP10 and GEXP07 antibodies confirmed our flow cytometry and immune fluorescence analysis, showing that in mature asexual stages and immature gametocytes a majority of antigen remains inside the RBC (**Figure 1F and S2**). Interestingly, a major pool of antigen also accumulated internally in mature gametocyte, however the role of these antigens in gametocytes or the resulting gametes remains to be determined. Altogether these

data confirmed and extended our previous observations (Dantzler et al, 2019), demonstrating reversible iRBC surface exposure of parasite antigens peaking at stage II gametocytes.

Reversible PS flipping tracks with antigen exposure dynamics

In asexual parasites, antigen surface exposure peaks in schizonts, i.e., right before the asexual cycle ends. In contrast, the peak of antigen surface exposure in gametocytes is at stage II and hence must be reversible. This reversible dynamic during gametocyte development may be the result of major membrane remodelling to remove parasite antigens from the iRBC surface. To test this hypothesis, we quantified phosphatidylserine (PS) surface exposure during gametocyte development. Healthy RBCs maintain membrane lipid asymmetry between the inner and outer leaflet: typically phosphatidylcholine (PC) and sphingomyelin (Sph) are located on the outer surface, while phosphatidylethanolamine (PE) and phosphatidylserine (PS) are located exclusively internally (Gordesky & Marinetti, 1973). Aged and damaged RBCs undergo eryptosis where PS is expressed on the outer surface, signalling macrophages to internalise and remove the damaged cells from circulation. Similarly, iRBCs expose PS on the outer leaflet of the host cell membrane in mature asexual stages (Fraser *et al.*, 2021a), because the parasite disrupts the maintenance of membrane asymmetry during schizogony (reviewed in (Fraser *et al*, 2021b)). To investigate whether PS becomes exposed on the iRBC surface during gametocyte development, we carried out a time course experiment and quantified Annexin V binding to surface exposed PS on intact iRBCs. Annexin V binding started in early gametocyte development, peaking at stage II and waning in mature stages with lowest PS exposure in stage V (**Figure 2**). This pattern was observed in both the Pf2004 and NF54 parasite lines by live fluorescence imaging (**Figure 2A**) and flow cytometry (**Figure 2B**). In NF54, we observed a much steeper decline in PS exposure at stage IV-V, possibly due to the difference in stage IV-V maturation between the two parasites lines (**Figure 2B).** Using a specific PS antibody, we noted little change in internal PS staining, in contrast to the reversible surface dynamics (**Figure 2D**). Altogether these data revealed a reversible exposure of PS to the iRBC surface during gametocyte development. Importantly, our observations suggest that parasite surface antigen exposure

and iRBC membrane remodelling coincide during early gametocyte development before both processes are reversed at later stages.

Blocking antigen surface expression also affects PS flipping

The similar dynamics of reversible surface antigen exposure and PS flipping also suggested that the two processes may be interlinked. This hypothesis was supported by the strong positive correlation between surface antigen exposure and PS flipping across individual samples **(Figure 3A)**. To directly test this hypothesis, we used specific perturbations targeting each process individually. The *P. falciparum* protein export pathway, including processing of exported proteins by the aspartyl protease, Plasmepsin V (PMV) (reviewed in (Maier *et al*, 2009)) is operational in asexual and gametocyte stages (Jennison *et al*, 2019). To determine whether PMV affects iRBC surface expression during gametocyte development we utilized an inhibitor of PMV (WEHI 842) (Hodder *et al*, 2015; Sleebs *et al*, 2014) in the background of the Pf2004/Tdtom-Gexp02/GFP dual reporter line. When added at gametocyte ring stage (10-16 hpi) the PMV inhibitor affected early gametocyte development in a concentration dependent manner (**Figure 3B-C**), as previously reported (Jennison *et al*., 2019). Using the Tdtom reporter signal intensity as a proxy for stage development, we noted that a minor proportion of gametocytes was not arrested and instead developed normally at lower drug concentrations (1 and 2 μM) (**Figure 3D)**. Gating for this subset of developing gametocytes, we then used the Gexp02/GFP reporter to test whether the PMV inhibitor blocked GEXP02 export. Indeed, our data demonstrate that export is reduced at 2 μM in immature gametocytes (**Figure 3E)**. Further experiments using the same gating strategy and 2 μM of drug also revealed a significant reduction in serum and GEXP10 antibody surface binding in asexual parasites (**Figure 3F)** and immature gametocytes (**Figure 3G)**. Conversely there was no effect on gametocyte development or GEXP10 export when the drug was added at stage II and later (**Figure 3H, I)**. However, we observed a significant reduction in serum surface labelling of mature gametocytes (**Figure 3I**), suggesting that some PMV dependent antigen export continues during gametocyte maturation.

Our observation of similar dynamics in surface antigen expression and PS surface exposure suggested shared underlying mechanisms. To test whether these two processes are interlinked, we investigated whether membrane remodelling is dependent on parasite antigen export. Specifically, we tested the effect of PMV inhibition on PS exposure during gametocyte development. Indeed, adding 2 μM of PMV inhibitor at gametocyte ring stages resulted in a significant reduction in PS exposure at stage II gametocytes (**Figure 3J**). In contrast, when PMV inhibitor was added at stage II gametocytes, PS surface exposure was not affected in late gametocyte development (**Figure 3K**). Altogether these data suggest that PS flipping in early gametocytes at least partially depends on an exported parasite activity, while the reverse process during later gametocyte maturation does not.

PS exposure and reversal can be blocked by scramblase inhibition

In a next series of experiments, we investigated the possible mechanisms underlying the reversible PS flipping on the iRBC surface. Recently, a *P. falciparum* phospholipid scramblase (*Pf*PL-SCR1, accession number PF3D7_1022700) with expression in late asexual stages and gametocytes was reported. Phospholipid scramblases are enzymes that translocate phospholipids across membranes in an ATP-dependent fashion. A *P*fPL-SCR1-GFP fusion protein localized to parasite internal membranes (**Figure 4A**), suggesting a role in PS scrambling in the parasite (Haase *et al*, 2021). Genetic deletion did not have an effect on parasite growth; however, PS exposure was not investigated in the original study. We hypothesized that this parasite scramblase could be involved in iRBC membrane remodelling. Deletion of the parasite scramblase in a *Pf*PL-SCR1 KO line resulted in significant reduction of PS exposure in late asexual stages and early gametocytes stages, while loss of surface PS in later stages was unaffected (**Figure 4B-F**). Interestingly, genetic deletion of the scramblase did not have an effect on surface antigen exposure (**Figure 4G**). Altogether these data demonstrate that the parasite scramblase is required for efficient PS flipping on the iRBC surface in asexual and early gametocyte stages, but not for the reversal during later gametocyte development.

To further investigate PS flipping on the iRBC surface during gametocyte development, we tested four mutually compatible scenarios: i) parasite-induced channels could cause a calcium influx affecting cell membrane scrambling and PS exposure (i.e. host flippase or scramblase activity (Fraser *et al.*, 2021a)) ; ii) high intracellular calcium levels could activate the Gardos channel (a host potassium channel) leading to KCL and water efflux and increased PS exposure (Tubman *et al*, 2016)) ; iii) increased cellular calcium could lead to translocation of host protein kinase Ca (PKCa) to the plasma membrane and further increase of calcium uptake (via host PKC and Syk kinase) (Wesseling *et al*, 2016) – a positive feedback mechanism inducing PS exposure; iv) inhibition of ATP hydrolysis could result in increased intracellular calcium and PS exposure, as has been shown in asexual iRBCs (Fraser *et al.*, 2021a). We used a series of commercially available inhibitors to test each of these scenarios individually: (i) flippase inhibitor (N-ethylmaleimide, NEM)(Vallabhapurapu *et al*, 2015) and scramblase inhibitor (Ethaninidothioic acid, R5421)(Millington-Burgess *et al*, 2020), ii) Gardos channel blocker (Senicapoc) (Tubman *et al.*, 2016), iii) PKCa inhibitor (Chelerythrine chloride, CHE) and tyrosine kinase (Syk) inhibitor (Ferru *et al*, 2011; Pantaleo *et al*, 2017), and iv) ATP hydrolysis inhibitor (Vanadate)(Fraser *et al.*, 2021a). To exclude a possible effect on parasite viability we tested each inhibitor in asexual parasites first, with the aim to select the highest non-toxic concentration (i.e., no effect on parasite multiplication rate, PMR) for subsequent assays in gametocytes **(Figure S3).** Titration series were set up, starting with concentrations from the studies referenced above. Parasites were treated at trophozoite stage and PS exposure by annexin V binding quantified at the mature schizont stage. PMR was quantified after one cycle of reinvasion at the next trophozoite stage (48hrs drug exposure). In asexual parasites, increasing concentrations of Syk and PKCa inhibitors reduced both surface PS exposure and PMR. In contrast, scramblase, flippase and Gardos channel inhibitors had no significant effect on PS exposure nor PMR in asexual parasites. Finally, we were not able to determine a non-toxic concentration for the ATP hydrolysis inhibitor (i.e., all concentrations tested significantly reduced parasite growth)(**Figure S3E)**. Based on these experiments we selected drug concentrations for single dose treatment in gametocytes. Specifically, for Syk and PKCa inhibitors we used the highest non-toxic concentration of 2.5 μM (i.e., no

significant effect on PMR). For the flippase inhibitor we used 20 μM, for the scramblase inhibitor 100 μM, and for the Gardos channel inhibitor we used the published IC50 concentration for *P. falciparum* of 6.7 μM. For vanadate we used 1.25 μM, the highest concentration that allowed some gametocyte development (all higher concentrations completely blocked growth). To measure an effect on PS surface exposure, inhibitor was added at early stage I gametocytes (3 days post induction) for 48 hours and PS surface exposure quantified at stage II gametocytes (5 days post induction). To measure an effect on surface PS internalisation, inhibitors were added at stage III gametocytes (6 days post induction) and surface PS measured at stage IV-V gametocytes. None of the inhibitors had any significant effect on PS surface flipping in stage II gametocytes (**Figure 5A**). In contrast, scramblase, flippase and ATP hydrolysis inhibitors significantly reduced PS internalisation in mature gametocytes (**Figure 5B**). However, both flippase and ATP hydrolysis inhibitors also blocked gametocyte development (**Figure 5C**), thus the observed effect on PS internalisation is likely the result of arrested or dying gametocytes. In conclusion, the only inhibitor that specifically affected PS surface internalisation was the non-specific scramblase inhibitor, R5421. This inhibition was specific to PS, while antigen surface expression or immune recognition of the iRBC surface remained unaffected (**Figure 5D)**. Altogether these data suggest that loss of PS exposure during gametocyte maturation depends on a host scramblase, and that process is independent of the loss of surface antigens.

Host cell remodelling impacts parasite clearance mechanisms by immune cells

We have previously demonstrated that immune sera from malaria patients can induce opsonic phagocytosis of gametocyte infected RBCs, suggesting that surface antigens elicit these immune responses. To further investigate the effect of surface antigen expression on gametocyte infected RBC clearance, a potential host immune mechanism of transmission reducing immunity, we measured antibody dependent opsonic phagocytosis using commercial THP-1 cells (Teo *et al.*, 2015), across gametocyte maturation. We observed significant phagocytosis of asexual and immature gametocyte, but not mature

gametocytes, when opsonized with immune sera (**Figure S4A**). Uptake of opsonized mature gametocytes was comparable to background phagocytosis observed when opsonized with non-immune sera. Addition of Plasmepsin V in these experiments reduced surface antigen exposure in asexual and immature gametocyte stages **(Figure S4B,C)** but did not result in reduced phagocytosis of either stage **(Figure 6A,B).** A recent study demonstrated that PS exposure leads to increased asexual iRBC uptake by monocytes (Fraser *et al.*, 2021a). Here we tested whether the reduced surface PS levels in the *Pf*PL-SCR1 KO line had any effect on asexual iRBC uptake by THP-1 cells. Indeed, we observed significantly decreased non-opsonic (i.e., serum-independent) phagocytosis of KO compared to wild type parasites (**Figure 6C**).

Finally, we determined whether blocking host scramblase activity in mature gametocytes impacted phagocytic clearance. We used the scramblase inhibitor R5421 to treat stage II gametocytes and block PS flipping off the iRBC surface (see **Figure 5**) and measured the effect on non-opsonic phagocytosis. This experiment revealed a significant increase in phagocytic uptake of treated mature gametocytes, similar to the effect in our positive control (**Figure 6D**). The observed effect was specifically due to surface PS because there was no effect on antibody-dependent opsonic phagocytosis (**Figure 6E**). Altogether these data suggest that phagocytosis of immature gametocytes is at least partially driven by PS exposure, and that blocking PS flipping represents a promising drug target to block transmission.

Discussion

P. falciparum has an unusually long gametocyte development compared to other *Plasmodium* species, during which the infected cell undergoes an extensive morphological transformation. Parasites export antigens onto the surface of host iRBCs during early gametocyte development in a similar trajectory as in the asexual stages. In both stages there is a gradual increase in surface antigen export starting around 20 hrs post invasion (late ring stages) and peaking in schizonts and stage II gametocytes, respectively. While

schizonts burst to release invasive daughter cells with a new set of surface antigens required for RBC invasion, antigens are actively removed from the iRBC surface before maturation in Stage V gametocytes.

The data from the current study corroborate our earlier observations that sampled part of the gametocyte maturation cycle (Dantzler *et al.*, 2019). We further demonstrate that the loss of antigens is restricted to the iRBC surface as internal pools do not decline with gametocyte maturation. The purpose of these internal antigen pools remains unclear, but we hypothesise that antigen export to the iRBC surface is tightly regulated to minimise antigen exposure to the host immune system. The internal antigen pool may also serve additional structural roles within the host RBC, as has been demonstrated for STEVOR antigens (Naissant *et al*, 2016). We also confirm that gametocytes rely on protein export via Plasmepsin V processing for surface antigen expression. Inhibition of PMV resulted in reduced stage II gametocyte surface recognition by serum and by antibodies to candidate gametocyte antigens GEXP07 and GEXP10. The incomplete block of surface recognition may be due to antigen export before PMV inhibitor treatment and/or the inhibitor concentration used. It is worth noting that at higher PMV inhibitor concentrations gametocyte development was greatly impeded (**Figure 3**). Nevertheless, blocking protein export in gametocytes provides an additional target for transmission blocking strategies by exposing maturing gametocytes both to splenic macrophages and other immune cells in peripheral circulation for clearance.

Importantly, our experiments reveal a dynamic change in lipid asymmetry during gametocyte maturation: whereas immature stages expose PS on the outer iRBC leaflet, mature stages do not. Uninfected RBCs and other mammalian cells generally maintain membrane lipid asymmetry with the anionic phospholipids PS and PE kept in the internal side facing the cytoplasm, while PC and SM are exposed externally to the cell environment. In homeostasis this heterogenous lipid distribution is maintained by three membrane integral phospholipid translocases, termed flippases, floppases, and scramblases (Hankins *et al*, 2015). Flippases are ATP-dependent and unidirectionally shunt PS and PE to the inner lumen of the membrane (Timcenko *et al*, 2019). Floppases are ABC-transporters that mediate the movement of phospholipids in the reverse direction (Coleman *et al*, 2013) while scramblases are

ATP-independent and act to randomize lipid distribution by bidirectionally translocating lipids between leaflets (Sahu *et al*, 2007). Disruption of this asymmetry signals cell damage and apoptosis, resulting in removal of the damaged cell. The hallmark of apoptosis is constitutive and non-reversible PS translocation to the outer surface of the cell membrane, which signals immune cells to clear the damaged cell. In the case of RBCs, the normal ageing process results in PS exposure and removal by splenic macrophages. Similarly, eryptosis due to RBC damage by oxidative or other cellular stresses involves PS exposure and subsequent phagocytosis of the damaged cell.

It has been hypothesised that *Plasmodium* (and a variety of other parasites) has adopted a strategy of non-classical apoptotic mimicry (Wanderley *et al*, 2020), where parasites induce apoptosis and co-opt the exposed PS of the apoptotic cell for its own survival, for instance by increasing the cytoadhesive capacity of the iRBC. PS exposure peaks in mature asexual stages and is important for merozoite egress (Fraser *et al.*, 2021a). Earlier work suggested that PS exposure on iRBCs facilitates binding to endothelial cells via interaction with CD36 and CXCCL16 (Closse *et al*, 1999; Manodori *et al*, 2000). Here we demonstrate that immature gametocytes expose PS on the iRBC surface, and that this exposure is reversed in mature gametocytes. The role of this remodelling is still unclear but as indicated for asexual parasites, we propose a role in cytoadhesion and sequestration. Cytoadhesive antigens remain elusive in gametocytes and therefore PS could play a more central role in mediating sequestration in the extravascular space of the bone marrow. Sexual stage parasites are generally considerably lower in abundance than their asexual counterparts and take longer to develop and mature in the host, and therefore they might require additional measures for immune evasion. The coincidental loss of PS and surface antigens is both a novel and logical observation, as it allows circulation of mature gametocytes without eliciting immune clearance responses.

PS exposure in immature gametocytes depends on a parasite phospholipid scramblase, *Pf*PL-SCR1, that localises to internal parasite membranes while exerting an effect on lipid asymmetry on the host cell membrane. This suggests a role for exported proteins in membrane lipid trafficking and remodelling, as supported by the sensitivity of PS exposure to PMV inhibitor treatment. The mechanism of PS exposure

by *Pf*PL-SCR1 is potentially similar in immature gametocytes and mature asexual stages (Fraser *et al.*, 2021a), while the removal in mature gametocytes occurs via an unknown mechanism clearly independent of *Pf*PL-SCR1. To investigate the mechanism of PS removal, we tested a series of compounds blocking possible modes of action including host flippases, scramblases, calcium channels and kinase signalling. None of the compounds affected either asexual or immature gametocyte PS exposure. In contrast, a scramblase inhibitor blocked PS removal in mature gametocytes (without affecting gametocyte development), suggesting that PS dynamics in maturing gametocytes are regulated by scramblase activity. Altogether, our observations that a combination of host and parasite scramblases is required for membrane lipid remodelling in gametocytes provide novel insights into the intricate mechanisms of host-parasite interactions in *Plasmodium* (**Figure 6F**).

Developing anti-gametocyte approaches is key to eliminating malaria. Gametocytes are the only transmissible stages and blocking this stage will play a significant role in elimination strategies, especially when transmission has been brought down by other preventative public health measures like intensive vector control. Whilst transmission-blocking interventions have traditionally focused on blocking parasite development inside mosquitoes, anti-gametocyte interventions can be equally potent and have the operational advantage that their effectiveness can be confirmed by monitoring gametocyte carriage in human populations. Indeed, our phagocytosis data provide a proof-of-concept for the development of novel intervention strategies that either inhibit gametocyte sequestration by blocking antigen and/or PS exposure, or by inducing splenic clearance of circulating gametocytes by blocking PS and/or antigen removal. We did not observe an effect of the PMV inhibitor on phagocytosis of asexual stages and immature gametocytes. However, the inhibitor efficiently blocks antigen surface exposure, and the level of surface exposure is strongly correlated with the level of phagocytosis (Dantzler *et al.*, 2019). It is therefore likely that a putative effect of PMV inhibitor on iRBC phagocytosis is masked by an unknown off-target activity that triggers phagocytosis independent of parasite antigen exposure. In contrast, incubating immature gametocytes with the host scramblase inhibitor R5421 resulted in efficient phagocytosis of mature gametocytes due to the inhibition of PS flipping off the iRBC surface. These data

suggest that targeting the host RBC scramblase can block parasite transmission by increasing splenic clearance, offering a new approach for host targeted therapies in the fight against malaria. Altogether, our data provide a foundation for further mechanistic studies and targeted approaches for novel transmission blocking therapeutics.

Materials and methods

Immune serum samples and ethical approval

Archived sera samples from Malawi and Tanzania were used as highly reactive pools for immune assays. Sera from Malawi were collected as previously described (Dantzler *et al.*, 2019), from 3 district hospitals (Ndirande, Thyolo, Chikhwawa) in the region of Blantyre, Malawi. Sample were collected by staff from the International Center of Excellence for Malaria Research (ICEMR) surveillance study after written informed consent was obtained from participants and/or their parent(s) or guardian(s). The project was approved by IRB boards of Harvard T.H. Chan School of Public Health, University of Malawi College of Medicine, Michigan State University, and University of Maryland. Tanzanian immune sera were collected as described in (Drakeley *et al*, 2006). Naïve sera controls were obtained from Interstate Blood Bank (Memphis, TN, USA) or Radboud University Medical Centre (Nijmegen, the Netherlands).

Transgenic parasites generation

Generation of GEXP02 (PlasmoDB: PF3D7_1102500) GFP-tagged parasite lines: To generate Pf2004/0164Tdt line the pB_gC Cas9/sgRNA plasmid (ref) was modified to generate pBgC-GEXP02 as follows. Two complementary oligonucleotides (G02GFP_gRNA_fwd and G02GFP_gRNA_rev) encoding the sgRNA target sequence for GEXP02 and appropriate single-stranded overhangs were annealed and inserted into the sgRNA expression cassette using *Bsa*I-digested pB_gC and In-Fusion cloning. The donor cassette was generated using In-Fusion ® HD cloning kit (Takara) to join PCR fragments GEXP02 homology region (HR) 1 amplified from Pf2004_164Tdtom gDNA using primers G02GFP_HR1_fwd and G02GFP_HR1_rev, and GEXP02 HR2 generated using primers

G02GFP_HR2_fwd and G02GFP_HR2_rev. PCR was performed with Phusion HF DNA polymerase (NEB) with the following thermocycling conditions: initial denaturation at 95°C for 2 min, thermocycling with denaturation at 95°C for 30 sec, annealing gradient ramp from at 45°C to 55°C for 30 sec, elongation at 61°C for 1 min for 8 cycles, 22 additional cycles [denaturation at 95°C for 30 sec, annealing at 55°C for 30 sec, elongation at 61°C for 1 min] and final elongation step at 61°C for 8 min. In the edited strain (Pf2004/164tdTom –GEXP02-GFP), integration of *bsd* resistance marker was verified by PCR using primers G02KO_INT_fwd and BSD_5'UTR_R primer (testing 5' integration) and BSD_3'UTR_F and 3'INT G02 GFP rev (testing 3' integration). PCR conditions were as follows: initial denaturation at 95°C for 2 min, thermocycling with denaturation at 95°C for 30 sec, annealing at 48°C for 30 sec, and elongation at 61°C for 1 min for 25 cycles, and final elongation step at 61°C for 8 min. All oligonucleotide sequences are provided in supplementary table 1.

Pf2004/164tdTom ring stage parasites were transfected with 100 µg of the plasmid above using electroporation as previously described (Buchholz *et al*, 2011). To select for parasites carrying the plasmids, transfected parasites were grown in presence of 2.5 µg/ml blasticidin-S deaminase for the first 10 days and then in absence of drug pressure until a stably propagating parasite population was established (approximately 4 weeks post-transfection). Clones of transgenic parasites were generated by serial dilution (Rosario, 1981). Successful integration in the transfected parasite population was confirmed by PCR on gDNA extracted using DNeasy blood and tissue kit (Qiagen), with primers listed in (Table of primers).

P. falciparum in vitro culture and gametocyte induction

Strains used in this study were NF54 (Nijmegen, the Netherlands) and Pf2004, originally from Ghana (Elliott *et al*, 2005). The transgenic parasite lines NF54- and Pf2004-164TdTomato expresses the tandem red fluorescent protein TdTomato under the control of an early gametocyte promoter (Aingaran *et al.*, 2012; Brancucci *et al*, 2015; Buchholz *et al.*, 2011) and requires addition of 4 nM WR99210 (Jacobus

Pharmaceuticals) to culture to maintain the transgene. Transgenic lines, GEXP02-GFP reporter lines were used for time course studies to track the earliest stages of gametocytogenesis (Portugaliza *et al.*, 2019). The 3D7 WT, *Pf*PL-SCR1-KO and *Pf*PL-SCR1-GFP tagged lines were generously gifted by the Baum lab (Haase *et al.*, 2021).

Plasmodium falciparum parasites were grown *in vitro* as previously described (Trager & Jensen, 1976) in fresh type O+ human erythrocytes (NHS), suspended at 5% haematocrit. Culture media was composed of HEPES-buffered RPMI 1640 0.05% gentamycin, 0.0201% sodium bicarbonate (w/v) and 0.005% hypoxanthine (w/v) at pH 6.74. Serum media was supplemented with 10% human serum (Interstate Blood Bank), while serum-free medium (MFA) was prepared as previously described (Brancucci *et al*, 2017) by additional supplementation of 0.39% fatty acid-free BSA, 30 μM oleic acid, and 30 μM palmitic acid (all from Sigma-Aldrich). Cultures were kept at 37°C in a gassed chamber at 5% CO_2 and 1% O_2.

Gametocytes were produced as previously described (Brancucci *et al.*, 2015). Briefly, parasites were double synchronised using 5% sorbitol to within an 8-hour window and seeded at 1.5–2% parasitemia and 5% hematocrit. Serum media was replaced with MFA with when the cultures were between 20-30hpi. Cultures were returned to serum media after 20hrs incubation with MFA. hours, after which the cultures were returned to serum medium. Beginning 24 hours after serum medium replacement, media was changed every day with addition of heparin (230ug/ml) for 2 consecutive days to completely block reinvasion and deplete the asexual stages. Parasite development and conversion was observed by daily smearing. For time course experiments gametocytes were harvested on a daily or on alternative days for 10-11 days to capture the different morphological forms, a typical time course being day 3-4 days post invasion (4-5 days post induction) for stage I/II; day 5-6 stage II/III; day 7-8 stage III/IV and day 9-11 stage V gametocytes. On days 8-11 E64 at 10uM final concentration was added to culture media to prevent gamete activation.

iRBC enrichment by Magnetic-activated cell sorting (MACS)

We utilized the QuadroMACS™ or MACS midi system (Miltenyi Biotec, Bergisch Gladbach, Germany) to enrich for iRBCs (mature asexual stages and all gametocyte stages) following a modified protocol (Ribaut *et al*, 2008). Cultures were washed once in incomplete RPMI, resuspended to 50% hematocrit and applied to MACS LD column pre-loaded with RPMI. Gametocytes and mature asexual parasites retained in the column were eluted with incomplete RPMI and washed 3x with RPMI. Following purification, cells were counted using a hemocytometer and aliquoted for downstream assays.

Flow cytometry

Flow cytometry was used to measure antibody binding to the surface of live iRBCs. 96-well plates were pre-coated with FACS buffer (1X PBS with 1% heat-inactivated foetal bovine serum (FBS) and 2mM EDTA) for 1 hour at room temperature or overnight at 4^0C, to prevent non-specific binding. Aliquots of purified asexual stage trophozoites or gametocytes (resuspended in 1X PBS) were pre-incubated for 1 hr with test primary antibodies, simultaneously with glycophorin C (2ug/mL) conjugated with Alexafluor 488 (1:500). Secondary antibodies (goat anti-rabbit IgG and goat anti-mouse diluted 1:500) were added to the cells and incubated for 30 min at room temperature. Nucleus dye Vybrant DyeCycle Violet™ diluted 1:500 or Hoechst diluted 1:1000 (Thermo Fisher Scientific) was then added to the cells and incubated at 37°C for 30 min. The volume of each well was increased to 200uL. Plate was centrifuged at 1500rpm for 5 min and washed 3 times with 1% FACS buffer between every staining/incubation stages. All samples were tested in triplicate.

FACS data acquisition and analysis were performed on BD FACSCelesta (BD Biosciences, NJ, USA) or MACSQuant (Miltenyi). Events were acquired to allow analysis of a minimum of 5000 infected cells per sample. Data were analysed with FlowJo software. Samples were displayed in a bivariate plot of side scatter area vs forward scatter area to gate for intact cells and forward scatter area vs height to gate for singlets. Nucleus stain was used to gate for iRBCs and TdTomato (0164/TdTomato lines), mScarlet or GFP (GEXP02 lines) was used to gate for gametocytes. Data was displayed as either frequency of IgG

positive cells or geometric mean fluorescence intensity (MFI), corrected for background signal from secondary only cell staining.

Immunofluorescence microscopy

The same antibody combinations and incubations were used for live immunofluorescence. After staining and washing, cells were mounted onto Concanavalin A (Sigma) coated hydrophobic printed well slides (EMS, 63425-05) with Vectashield (Vector Labs, Burlingame, CA, USA).

For fixed and permeabilised IFA, MACS purified mature asexual stages (36-44hpi) or gametocyte stages were washed 3x in PBS and subjected to trypsin/chymotrypsin treatment as above. Cells were fixed for 40 min in 4% paraformaldehyde/0.01% glutaraldehyde, washed 3x in PBS, permeabilized for 10 min using 0.1% Triton-X and washed 3x. CBPI and CBPII antibodies or SBP-1 antibody (N-terminal rabbit, kindly provided by Dr. Tobias Spielmann) were then incubated with trypsin/chymotrypsin-treated or mock-treated iRBCs at 0.4% hematocrit, and surface binding was detected using Alexa Fluor® 488 anti-IgG dye (Thermo Fisher Scientific; 1:500). Nucleus staining was done using DAOI or Hoechst. After all incubations washes were carried out with PBS supplemented with 1% FBS. Cells were mounted with Vectashield (Vector Labs, Burlingame, CA, USA). Images were obtained under a 60X objective using Nikon A1R inverted confocal microscope. Images and movies were generated using Image J software 2.9.0/1.53t.

Phagocytosis assay

Phagocytosis assays were performed as previously described (Dantzler *et al.*, 2019; Teo *et al.*, 2015). Briefly, the assay measures phagocytic uptake of iRBCs via opsonic antibodies and Fcγ receptors on undifferentiated THP-1 cells (European collection of authenticated cell cultures), which do not express CD36 and therefore do not promote non-opsonic phagocytosis. THP-1 cells were maintained in THP-1 culture medium at 5 x 10^5 cells/ml in a humidified incubator at 37°C supplemented with 5 % CO_2. iRBCs (mature asexual stages or gametocytes) were MACS purified and stained with 10 mg/ml dihydroethidium

(DHE)(Sigma- Aldrich) for 30 minutes in the dark (RT). Cells were washed thrice with RPMI and adjusted to a cell density of 8.25 x 10^6 cells/ml. For opsonization test sera (3.3 µL) followed by 30 µL iRBC suspension was added in triplicate to 96-well plates previously incubated with heat-inactivated new-born calf serum. For non-opsonized phagocytosis cells were kept in RPMI. Rabbit anti-RBC antibody (Abcam ab34858) was used a positive control (1:100). After 1 hour of opsonization at RT, cells were washed thrice with RPMI, re-suspended in 25 µL THP-1 medium and aliquoted into new plates (pre-incubated with NCS). 50 µL of THP-1 cells (5 x 10^5 cells/ml) were then added to each well and the plate was incubated for 40 min at 37 °C in a CO^2-supplemented humidified incubator. After phagocytosis, the plate was centrifuged at 350 x g for 5 minutes at 4°C. The supernatant was removed and 75 µL FACS lysing solution (BD Biosciences) was added for 10 minutes (RT). The plate was then spun down (4°C) and washed thrice with FACS buffer. Cells were filtered before acquisition on a MACSQuant Analyzer flow cytometer (Miltenyi Biotec) or imaged on the Nikon confocal microscope. After gating for live cells based on forward/side scatter, a gate for positive DHE fluorescence was set based on <5% cells of the negative control (no sera added). Phagocytic index (percentage of THP-1 cells that phagocytosed iRBCs) for each sample was then determined by subtracting average negative control fluorescence and dividing by average positive control fluorescence.

Immunoelectron microscopy

For immunolabeling, the samples were fixed in phosphate buffer, pH 7.2, containing 4% freshly prepared formaldehyde. After several washes in the same buffer, they were dehydrated in ascending ethanol series and embedded in LR White resin (Agar Scientific). Ultrathin sections (70 nm thick) were obtained using an ultramicrotome (Leica Microsystems). The sections were collected on formvar-coated nickel grids and then blocked in PBS containing 3% bovine serum albumin for 1 hour. After this time, they were incubated in the presence of primary antibodies (anti-CBPI and anti-CBPII). Then they were washed several times in blocking buffer and incubated with 10 or 15 nm gold-conjugated Protein A (Aurion). The grids were washed several times in the blocking buffer, dried and contrasted with 4% uranyl acetate, and

observed using a JEOL 1200 EX transmission electron microscope operating at 80kV. Gold particles were quantified by eye as a measure of antigen labelling by the respective antibodies.

Annexin V binding

250,000 cells or less of purified mature asexual parasites, gametocytes, unpurified rings and uninfected RBCs were used in the assay. Briefly, cells were washed 3 times in RPMI and stained Hoechst (1:1000/ 20uM) for 15 minutes at room temperature. Stained cells were washed 2 times with annexin V buffer (130-092-820 Miltenyi) and resuspended in 25ul of annexin V buffer. 2.5ul Annexin V-FITC or Annexin V-AF647 was added to each sample and incubated for 15 minutes at room temperature in the dark. The cells were washed twice with 200ul Annexin V buffer, resuspended in 100ul Annexin V buffer and run on flow cytometer or mounted on glass dishes for imaging as described above.

Inhibition assay

PMV treatment

To block protein export at the onset parasites were exposed to the inhibitor WEHI-842 for 48 hours starting at the ring stages (asexual rings or gametorings) before 16hpi. To block protein export in maturing gametocytes parasite were exposed to WEHI-842 at stage II (day 5) for 48 hours. Read outs were performed at mature asexual stages, stage II and stage IV-V gametocytes.

PS exposure inhibitors

To test inhibitors that block PS surface flipping during asexual schizogony trophozoite stage parasites were incubator with complete media containing serial dilutions of the inhibitors for <20 hours. A subset of parasites was MACS purified at schizonts at >40hpi to measure annexin V binding by flow cytometry. The remaining subset was let to reinvade and mature for 24 hours to quantify parasite multiplication rate (PMR) post inhibitor treatment. To block PS surface flipping at stage II gametocytes parasite were treated with the inhibitors on day 3 post induction (gametotrophs- early stage I gametocytes) for 2 consecutive days. Readout by flow cytometry was carried out on day 5 post induction at stage II gametocytes. To

block the reversal of PS surface exposure stage II-III gametocytes (day 6 post invasion) were treated with the inhibitors for 2 consecutive days. Readout by flow cytometry was carried out on day 8-9 post induction at stage IV-V gametocytes. For all the experiments above the following readouts were made, (i) % positive annexin V for PS surface detection, (ii) immune sera and the antibodies CBPI and CBPII to measure effect of inhibitors on surface antigen exposure. For one inhibitor, R5421 a further sample of the treated stage II gametocytes was allowed to mature to stage IV to measure any late effect of the inhibitor on loss of surface antigens (**Figure 5E**).

Acknowledgements

This work was supported by ERC Consolidator award BoneMalar (PN, KDP, MP, MM), ERC Consolidator award 864180 (TB), MRC Programme grant MR/T016272/1 (PN, MP, MM, TB), Royal Society Wolfson Merit Award (MM), Wellcome Trust Center award 104111 (PN, KDP, MP, MM) and NIH ICEMR grant U19AI129388 (TT). We would like to thank Alexander Maier (ANU, Canberra) for helpful discussions and advice, Philippe Deterre (INSERM, Paris) for CBP antibodies, Jake Baum (UNSW, Sydney) for *Pf*PL-SCR1-KO and *Pf*PL-SCR1-GFP parasite lines and Leandro Lemgruber (Glasgow Imaging Facility, University of Glasgow) for electron microscopy experiments.

References

Aingaran M, Zhang R, Law SK, Peng Z, Undisz A, Meyer E, Diez-Silva M, Burke TA, Spielmann T, Lim CT *et al* (2012) Host cell deformability is linked to transmission in the human malaria parasite Plasmodium falciparum. *Cell Microbiol* 14: 983-993

Bengtsson D, Sowa KM, Salanti A, Jensen AT, Joergensen L, Turner L, Theander TG, Arnot DE (2008) A method for visualizing surface-exposed and internal PfEMP1 adhesion antigens in Plasmodium falciparum infected erythrocytes. *Malaria journal* 7: 101

561 Brancucci NM, Goldowitz I, Buchholz K, Werling K, Marti M (2015) An assay to probe Plasmodium
562 falciparum growth, transmission stage formation and early gametocyte development. *Nat Protoc* 10:
563 1131-1142
564 Brancucci NMB, Gerdt JP, Wang C, De Niz M, Philip N, Adapa SR, Zhang M, Hitz E, Niederwieser I,
565 Boltryk SD *et al* (2017) Lysophosphatidylcholine Regulates Sexual Stage Differentiation in the Human
566 Malaria Parasite Plasmodium falciparum. *Cell* 171: 1532-1544 e1515
567 Buchholz K, Burke TA, Williamson KC, Wiegand RC, Wirth DF, Marti M (2011) A high-throughput
568 screen targeting malaria transmission stages opens new avenues for drug development. *J Infect Dis* 203:
569 1445-1453
570 Closse C, Dachary-Prigent J, Boisseau MR (1999) Phosphatidylserine-related adhesion of human
571 erythrocytes to vascular endothelium. *British journal of haematology* 107: 300-302
572 Coleman JA, Quazi F, Molday RS (2013) Mammalian P4-ATPases and ABC transporters and their role in
573 phospholipid transport. *Biochimica et biophysica acta* 1831: 555-574
574 Dantzler KW, Ma S, Ngotho P, Stone WJR, Tao D, Rijpma S, De Niz M, Nilsson Bark SK, Jore MM,
575 Raaijmakers TK *et al* (2019) Naturally acquired immunity against immature Plasmodium falciparum
576 gametocytes. *Sci Transl Med* 11
577 De Niz M, Meibalan E, Mejia P, Ma S, Brancucci NMB, Agop-Nersesian C, Mandt R, Ngotho P, Hughes
578 KR, Waters AP *et al* (2018) Plasmodium gametocytes display homing and vascular transmigration in the
579 host bone marrow. *Sci Adv* 4: eaat3775
580 Drakeley CJ, Bousema JT, Akim NI, Teelen K, Roeffen W, Lensen AH, Bolmer M, Eling W, Sauerwein
581 RW (2006) Transmission-reducing immunity is inversely related to age in Plasmodium falciparum
582 gametocyte carriers. *Parasite immunology* 28: 185-190
583 Elliott SR, Duffy MF, Byrne TJ, Beeson JG, Mann EJ, Wilson DW, Rogerson SJ, Brown GV (2005)
584 Cross-reactive surface epitopes on chondroitin sulfate A-adherent Plasmodium falciparum-infected
585 erythrocytes are associated with transcription of var2csa. *Infection and immunity* 73: 2848-2856

586 Ferru E, Giger K, Pantaleo A, Campanella E, Grey J, Ritchie K, Vono R, Turrini F, Low PS (2011)
587 Regulation of membrane-cytoskeletal interactions by tyrosine phosphorylation of erythrocyte band 3.
588 *Blood* 117: 5998-6006
589 Fraschka SA, Filarsky M, Hoo R, Niederwieser I, Yam XY, Brancucci NMB, Mohring F, Mushunje AT,
590 Huang X, Christensen PR *et al* (2018) Comparative Heterochromatin Profiling Reveals Conserved and
591 Unique Epigenome Signatures Linked to Adaptation and Development of Malaria Parasites. *Cell host &*
592 *microbe* 23: 407-420 e408
593 Fraser M, Jing W, Broer S, Kurth F, Sander LE, Matuschewski K, Maier AG (2021a) Breakdown in
594 membrane asymmetry regulation leads to monocyte recognition of P. falciparum-infected red blood cells.
595 *PLoS Pathog* 17: e1009259
596 Fraser M, Matuschewski K, Maier AG (2021b) Of membranes and malaria: phospholipid asymmetry in
597 Plasmodium falciparum-infected red blood cells. *Cell Mol Life Sci* 78: 4545-4561
598 Gordesky SE, Marinetti GV (1973) The asymetric arrangement of phospholipids in the human erythrocyte
599 membrane. *Biochem Biophys Res Commun* 50: 1027-1031
600 Haase S, Condron M, Miller D, Cherkaoui D, Jordan S, Gulbis JM, Baum J (2021) Identification and
601 characterisation of a phospholipid scramblase in the malaria parasite Plasmodium falciparum. *Molecular*
602 *and biochemical parasitology* 243: 111374
603 Hankins HM, Baldridge RD, Xu P, Graham TR (2015) Role of flippases, scramblases and transfer
604 proteins in phosphatidylserine subcellular distribution. *Traffic* 16: 35-47
605 Hawking F, Wilson ME, Gammage K (1971) Evidence for cyclic development and short-lived maturity in
606 the gametocytes of Plasmodium falciparum. *Transactions of the Royal Society of Tropical Medicine and*
607 *Hygiene* 65: 549-559
608 Hentzschel F, Gibbins MP, Attipa C, Beraldi D, Moxon CA, Otto TD, Marti M (2022) Host cell
609 maturation modulates parasite invasion and sexual differentiation in Plasmodium berghei. *Sci Adv* 8:
610 eabm7348

611 Hermand P, Ciceron L, Pionneau C, Vaquero C, Combadiere C, Deterre P (2016) Plasmodium falciparum
612 proteins involved in cytoadherence of infected erythrocytes to chemokine CX3CL1. *Sci Rep* 6: 33786
613 Hodder AN, Sleebs BE, Czabotar PE, Gazdik M, Xu Y, O'Neill MT, Lopaticki S, Nebl T, Triglia T,
614 Smith BJ *et al* (2015) Structural basis for plasmepsin V inhibition that blocks export of malaria proteins
615 to human erythrocytes. *Nat Struct Mol Biol* 22: 590-596
616 Jennison C, Lucantoni L, O'Neill MT, McConville R, Erickson SM, Cowman AF, Sleebs BE, Avery VM,
617 Boddey JA (2019) Inhibition of Plasmepsin V Activity Blocks Plasmodium falciparum
618 Gametocytogenesis and Transmission to Mosquitoes. *Cell reports* 29: 3796-3806 e3794
619 Joice R, Nilsson SK, Montgomery J, Dankwa S, Egan E, Morahan B, Seydel KB, Bertuccini L, Alano P,
620 Williamson KC *et al* (2014) Plasmodium falciparum transmission stages accumulate in the human bone
621 marrow. *Sci Transl Med* 6: 244re245
622 Kho S, Qotrunnada L, Leonardo L, Andries B, Wardani PAI, Fricot A, Henry B, Hardy D, Margyaningsih
623 NI, Apriyanti D *et al* (2021a) Evaluation of splenic accumulation and colocalization of immature
624 reticulocytes and Plasmodium vivax in asymptomatic malaria: A prospective human splenectomy study.
625 *PLoS Med* 18: e1003632
626 Kho S, Qotrunnada L, Leonardo L, Andries B, Wardani PAI, Fricot A, Henry B, Hardy D, Margyaningsih
627 NI, Apriyanti D *et al* (2021b) Hidden Biomass of Intact Malaria Parasites in the Human Spleen. *N Engl J*
628 *Med* 384: 2067-2069
629 Lee RS, Waters AP, Brewer JM (2018) A cryptic cycle in haematopoietic niches promotes initiation of
630 malaria transmission and evasion of chemotherapy. *Nat Commun* 9: 1689
631 Maier AG, Cooke BM, Cowman AF, Tilley L (2009) Malaria parasite proteins that remodel the host
632 erythrocyte. *Nat Rev Microbiol* 7: 341-354
633 Manodori AB, Barabino GA, Lubin BH, Kuypers FA (2000) Adherence of phosphatidylserine-exposing
634 erythrocytes to endothelial matrix thrombospondin. *Blood* 95: 1293-1300
635 Millington-Burgess SL, Bonna AM, Rahman T, Harper MT (2020) Ethaninidothioic acid (R5421) is not a
636 selective inhibitor of platelet phospholipid scramblase activity. *Br J Pharmacol* 177: 4007-4020

637 Naissant B, Dupuy F, Duffier Y, Lorthiois A, Duez J, Scholz J, Buffet P, Merckx A, Bachmann A,
638 Lavazec C (2016) Plasmodium falciparum STEVOR phosphorylation regulates host erythrocyte
639 deformability enabling malaria parasite transmission. *Blood* 127: e42-53
640 Obaldia N, 3rd, Meibalan E, Sa JM, Ma S, Clark MA, Mejia P, Moraes Barros RR, Otero W, Ferreira
641 MU, Mitchell JR *et al* (2018) Bone Marrow Is a Major Parasite Reservoir in Plasmodium vivax Infection.
642 *MBio* 9
643 Pantaleo A, Kesely KR, Pau MC, Tsamesidis I, Schwarzer E, Skorokhod OA, Chien HD, Ponzi M,
644 Bertuccini L, Low PS *et al* (2017) Syk inhibitors interfere with erythrocyte membrane modification
645 during P falciparum growth and suppress parasite egress. *Blood* 130: 1031-1040
646 Portugaliza HP, Llora-Batlle O, Rosanas-Urgell A, Cortes A (2019) Reporter lines based on the gexp02
647 promoter enable early quantification of sexual conversion rates in the malaria parasite Plasmodium
648 falciparum. *Scientific reports* 9: 14595
649 Ribaut C, Berry A, Chevalley S, Reybier K, Morlais I, Parzy D, Nepveu F, Benoit-Vical F, Valentin A
650 (2008) Concentration and purification by magnetic separation of the erythrocytic stages of all human
651 Plasmodium species. *Malaria journal* 7: 45
652 Rosario V (1981) Cloning of naturally occurring mixed infections of malaria parasites. *Science (New*
653 *York, NY* 212: 1037-1038
654 Sahu SK, Gummadi SN, Manoj N, Aradhyam GK (2007) Phospholipid scramblases: an overview. *Arch*
655 *Biochem Biophys* 462: 103-114
656 Silvestrini F, Lasonder E, Olivieri A, Camarda G, van Schaijk B, Sanchez M, Younis Younis S,
657 Sauerwein R, Alano P (2010) Protein export marks the early phase of gametocytogenesis of the human
658 malaria parasite Plasmodium falciparum. *Mol Cell Proteomics* 9: 1437-1448
659 Sleebs BE, Lopaticki S, Marapana DS, O'Neill MT, Rajasekaran P, Gazdik M, Gunther S, Whitehead
660 LW, Lowes KN, Barfod L *et al* (2014) Inhibition of Plasmepsin V activity demonstrates its essential role
661 in protein export, PfEMP1 display, and survival of malaria parasites. *PLoS biology* 12: e1001897

662 Teo A, Hasang W, Boeuf P, Rogerson S (2015) A Robust Phagocytosis Assay to Evaluate the Opsonic
663 Activity of Antibodies against Plasmodium falciparum-Infected Erythrocytes. *Methods Mol Biol* 1325:
664 145-152
665 Tiburcio M, Niang M, Deplaine G, Perrot S, Bischoff E, Ndour PA, Silvestrini F, Khattab A, Milon G,
666 David PH *et al* (2012a) A switch in infected erythrocyte deformability at the maturation and blood
667 circulation of Plasmodium falciparum transmission stages. *Blood* 119: e172-180
668 Tiburcio M, Silvestrini F, Bertuccini L, Sander AF, Turner L, Lavstsen T, Alano P (2012b) Early
669 gametocytes of the malaria parasite Plasmodium falciparum specifically remodel the adhesive properties
670 of infected erythrocyte surface. *Cellular microbiology*
671 Timcenko M, Lyons JA, Januliene D, Ulstrup JJ, Dieudonne T, Montigny C, Ash MR, Karlsen JL,
672 Boesen T, Kuhlbrandt W *et al* (2019) Structure and autoregulation of a P4-ATPase lipid flippase. *Nature*
673 571: 366-370
674 Trager W, Jensen JB (1976) Human malaria parasites in continuous culture. *Science* 193: 673-675
675 Tubman VN, Mejia P, Shmukler BE, Bei AK, Alper SL, Mitchell JR, Brugnara C, Duraisingh MT (2016)
676 The Clinically Tested Gardos Channel Inhibitor Senicapoc Exhibits Antimalarial Activity. *Antimicrobial*
677 *agents and chemotherapy* 60: 613-616
678 Vallabhapurapu SD, Blanco VM, Sulaiman MK, Vallabhapurapu SL, Chu Z, Franco RS, Qi X (2015)
679 Variation in human cancer cell external phosphatidylserine is regulated by flippase activity and
680 intracellular calcium. *Oncotarget* 6: 34375-34388
681 Wanderley JLM, DaMatta RA, Barcinski MA (2020) Apoptotic mimicry as a strategy for the
682 establishment of parasitic infections: parasite- and host-derived phosphatidylserine as key molecule. *Cell*
683 *Commun Signal* 18: 10
684 Warncke JD, Passecker A, Kipfer E, Brand F, Perez-Martinez L, Proellochs NI, Kooij TWA, Butter F,
685 Voss TS, Beck HP (2020) The PHIST protein GEXP02 targets the host cytoskeleton during sexual
686 development of Plasmodium falciparum. *Cellular microbiology* 22: e13123

687 Wesseling MC, Wagner-Britz L, Nguyen DB, Asanidze S, Mutua J, Mohamed N, Hanf B, Ghashghaeinia
688 M, Kaestner L, Bernhardt I (2016) Novel Insights in the Regulation of Phosphatidylserine Exposure in
689 Human Red Blood Cells. *Cell Physiol Biochem* 39: 1941-1954
690 WHO (2021) World malaria report 2021.
691

692 **Figure legends**

693 **Fig 1: Dynamics of surface antigen exposure in *P. falciparum* gametocytes**. **A, B.** Human serum
694 reactivity across asexual and gametocyte development by live microscopy and flow cytometry detection
695 in Pf2004 parasites. (**A**) Representative images of asexual and gametocytes after live labelling and
696 fluorescence microscopy using immune serum, and (**B**) flow cytometry quantification of the same
697 samples. **C, D.** Reactivity of GEXP10/CBPI antibodies in live cells by (**C**) fluorescence microscopy and
698 (**D**) flow cytometry. **E.** Human serum reactivity in PFA fixed (left) and PFA fixed and TX-100
699 permeabilized cells (right) in asexual and gametocyte stages. **F.** Quantification of antigen localization
700 based on immuno EM. Asexual stages: 24-36 hpi, GI-IIa: D4, GIIb-III: D6, GIII-IV: D8, GIV-V: D11.
701 Blue: DAPI, green: IgG, red: Tdtomato. **B**, and **D** represent the mean from three biological replicates. **F**,
702 counting a minimum of 30 images per stage and antibody.
703

704 **Figure 2. Reversible membrane remodelling tracks with antigen exposure during gametocyte**
705 **development**. **A-C**. Annexin V labelling in live MACS-enriched asexual and gametocyte stages by flow
706 cytometry (**A**: Pf2004, **B**: NF54) and fluorescence microscopy (**C:** Pf2004). **D.** PS staining using a
707 monoclonal anti-PS antibody in fixed and permeabilized asexual and gametocyte stages (Pf2004). Blue:
708 DAPI, green: Annexin V-FITC, red: Tdtomato, Magenta: anti-PS antibody-647. **A, B** represent the mean
709 from three biological replicates.
710

711 **Figure 3. Inhibition of antigen export blocks gametocyte development and surface recognition. A.**
712 Co-staining of surface labelling with human serum and PS with annexin V. Representative images of

713 asexual schizont (top) and stage II gametocytes (bottom). Graph showing correlation of surface labelling
714 and annexin V staining across individual samples (bottom panel). **B.** Flow cytometry data gating strategy.
715 Shown is an example for immature stage II gametocytes, day 5 post induction. Cell population was gated
716 to remove debris (i), followed by single event gating to remove doublets (ii). iRBCs were gated on
717 nuclear dye (iii) and gametocytes on Tdtomato (iv-vii). The Tdtomato % positive cells (gametocytemia)
718 varied based on PMV concentration. Left to right: DMSO control, 1uM PMV, 2uM PMV and 5uM PMV.
719 **C, D.** PMV inhibitor arrests early gam development at higher doses based on Tdt MFI quantification. **C**.
720 Quantification of gametocytemia in MACS enriched parasites by Tdtomato positivity across three PMV
721 inhibitor concentrations. **D**. Quantification of Tdtomato median fluorescence in Tdtomato positive cells
722 gated in C. **E**. PMV inhibitor at lower doses blocks antigen export in mature asexual stages (36-44hpi). **F**.
723 GEXP02 and TdTomato fluorescence upon PMV inhibitor incubation. PMV inhibitor at lower doses
724 blocks antigen export in immature gametocytes. Shown are representative images of immature
725 gametocytes (Stage II). **G.** Flow cytometry quantification of immune reactivity (human serum and CBPI)
726 upon PMV inhibitor incubation in immature gametocytes**. H-I.** PMV inhibitor has less effect on antigen
727 export in mature gametocytes. **H**. GEXP02 and TdTomato fluorescence upon PMV inhibitor incubation.
728 Shown are representative images of mature gametocytes (Stage IV-V). I. Quantification of immune
729 reactivity (human serum and CBPI) (**I**). **J, K. Annexin V staining upon** PMV inhibitor incubation in
730 immature gametocytes **(J**) and mature (**K**) gametocytes. Blue: DAPI, green: IgG (**A**)/ GEXP02-GFP
731 (**F,H**), red: Tdtomato. **C, D, E, G, I, J, K** represent the mean from three biological replicates.
732
733 **Figure 4. A *P. falciparum* scramblase affects PS surface exposure.** **A**. Localisation of *Pf*PL-SCR1-
734 GFP in relation to surface PS. **B-D**. Effect of *Pf*PL-SCR1 KO on PS exposure in schizonts **(B**), immature
735 (**C**) and mature (**D**) gametocyte stages. **E, F**. Representative images of PS staining in *Pf*PL-SCR1 KO
736 parasites using anti-PS antibodies. Shown are asexual schizont stages (**E**) and Stage II gametocytes (**F**).
737 **G**. Serum and antibody (CBP1 and CBPII) recognition in the *Pf*PL-SCR1 KO measured by flow

cytometry. Blue: DAPI, green: *Pf*PL-SCR1-GFP, Magenta: anti-PS antibody-647. **B, C, D, G** represent the mean from three biological replicates.

Figure 5. Blocking PS flipping in gametocytes using scramblase inhibitor. A. Single dose incubation of compounds tested for effect on immature gametocytes (Stage I-II). Concentration of compounds: NEM (20μM), R5421 (100μM), Senicapoc (6.7μM), CHE (2.5μM), Syk (2.5μM), Vanadate (1μM). **B**. Single dose of compounds tested for effect on mature gametocytes (Stage IV-V). Concentrations for all compounds as in **A**. **C**. Tdtomato reporter median fluorescence in mature gametocytes (Stage IV-V) to determine compound effect on gametocyte maturation. **D.** Effect of R5421 on human serum and CBP1 antibody surface recognition in immature and mature gametocytes. **A-D** represent the mean from three biological replicates.

Figure 6: Phagocytosis of iRBCs upon perturbations. A-B. Effect of PMV inhibitor on phagocytosis of asexual (A) and immature gametocyte (B) stages using immune serum vs US control serum for opsonisation. **C**. Effect of *Pf*PL-SCR1 KO PS exposure on iRBC phagocytosis in absence of serum (no opsonisation). Shown are asexual schizonts and ring stages. **D**. Effect of R5421 on Stage IV-V iRBC phagocytosis in absence of serum and upon addition of the calcium ionophore A23187. **E**. Effect of R5421 on Stage IV-V iRBC phagocytosis in presence of serum. **F**. A model of the remodelling process during gametocyte maturation and effect of the various perturbations**. A-E** represent the mean from three biological replicates. Phagocytosis index is determined by subtracting average negative control %DHE and dividing by average positive control %DHE.

Supplementary Figures

Figure S1. Dynamics of antigen exposure A. Flow cytometry detection of human serum reactivity in NF54. **B, C.** CBPI and CBPII surface reactivity in NF54. **D/E.** Reactivity of GEXP07/CBPII antibodies

against live Pf2004 cells by live microscopy (**D**) and flow cytometry (**E**). **A, B, C** and **E** and represent the mean from three biological replicates.

Figure S2. A major antigen pool remains internal in gametocytes. A. IFA data. GEXP10/CBPI surface labelling dynamics in fixed cells, internal labelling dynamics in fixed and permeabilized cells. **B.** Immuno EM data. A fraction of GEXP10 protein (CBPI) is present on the surface of asexual and gametocyte iRBCs. **C.** Image quantification of +/-Triton. Asexual (24-36hpi), GI-Iia (D4), GIIb-III (D6), GIII-IV (D8), GIV-V (D11). Panels show from top to bottom immune serum, GEXP10 (polyclonal antibody), CBPI/GEXP10 (monoclonal antibody), CBPII monoclonal antibody) reactivity. Blue: DAPI, green: IgG, red: Tdtomato. **C** represents the mean from three biological replicates.

Figure S3. Inhibition of membrane lipid remodelling affects antigen exposure and immune recognition. A-F. Testing various inhibitors to block PS exposure or internalization. **(A)** Syk inhibitor, **(B)** PKC alpha inhibitor (PKCa) – chelerythrine chloride, **(C)** Flippase inhibitor - NEM, **(D)** Senicapoc - Gardos channel inhibitor, **(E)** Vanadate - ATP inhibitor, **(F)** Scramblase inhibitor R5421 / oxalic acid dehydrate / ethanoininic acid. **A-F** represent the mean from three biological replicates.

Figure S4. Phagocytosis assays. A. Control experiment using asexual, immature and mature gametocyte stages. Opsonisation with immune serum (left) and with US control serum (right). **B, C.** Effect of PMV inhibitor on opsonisation of asexual stages and immature gametocytes using immune serum vs US control serum. Same samples as in Figure 6A and B respectively. **A-C** represent the mean from three biological replicates.

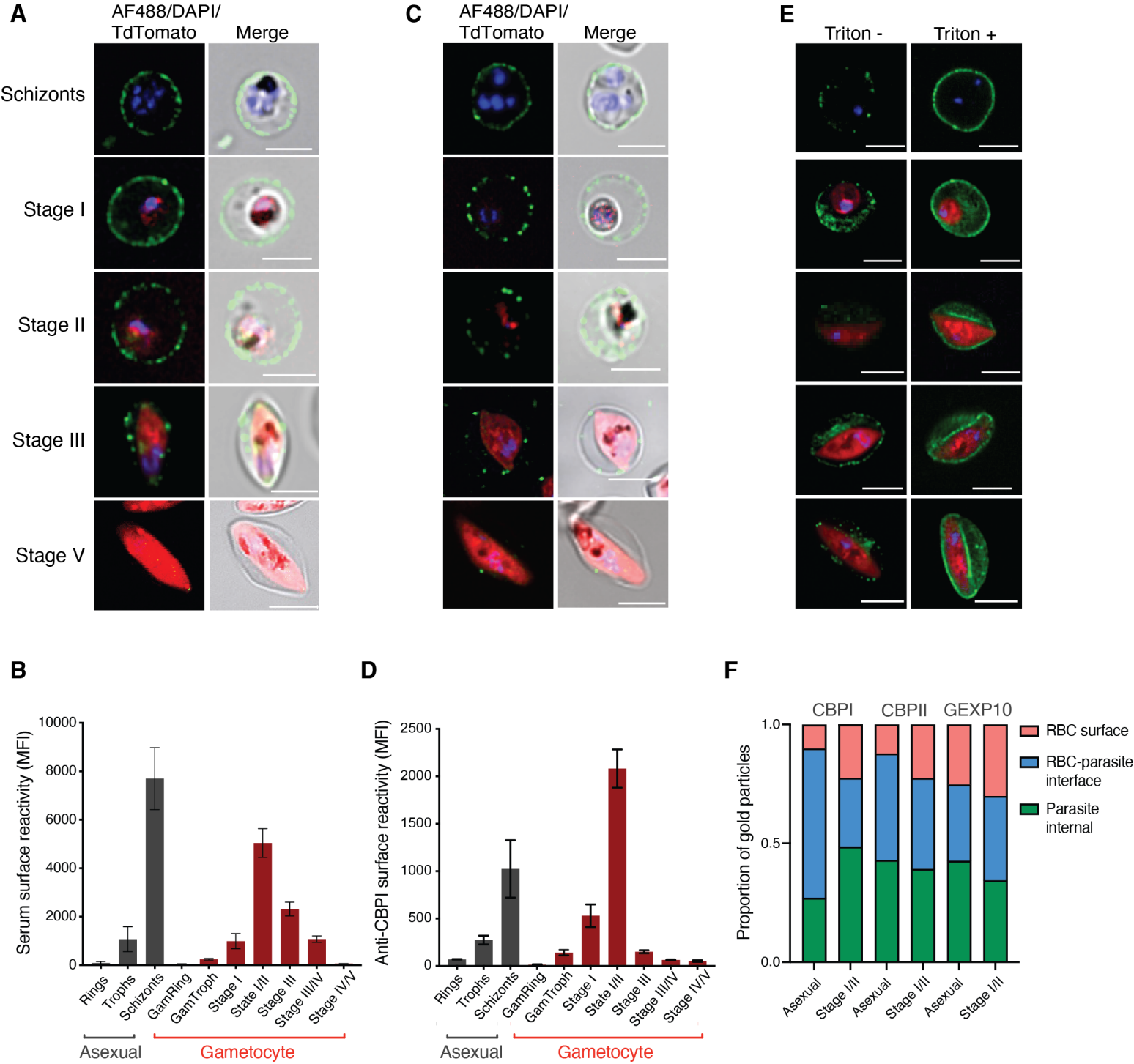
A
AF488/DAPI/
TdTomato
Merge
Schizonts
Stage I
Stage II
Stage III
Stage V
C
AF488/DAPI/
TdTomato
Merge
E
Triton -
Triton +
B
Serum surface reactivity (MFI)
10000
8000
6000
4000
2000
0
Rings
Trophs
Schizonts
GamRing
GamTroph
Stage I
State I/II
Stage III
Stage III/IV
Stage IV/V
Asexual
Gametocyte
D
Anti-CBPI surface reactivity (MFI)
2500
2000
1500
1000
500
0
Rings
Trophs
Schizonts
GamRing
GamTroph
Stage I
State I/II
Stage III
Stage III/IV
Stage IV/V
Asexual
Gametocyte
F
CBPI
CBPII
GEXP10
Proportion of gold particles
1.0
0.5
0.0
RBC surface
RBC-parasite interface
Parasite internal
Asexual
Stage I/II
Asexual
Stage I/II
Asexual
Stage I/II

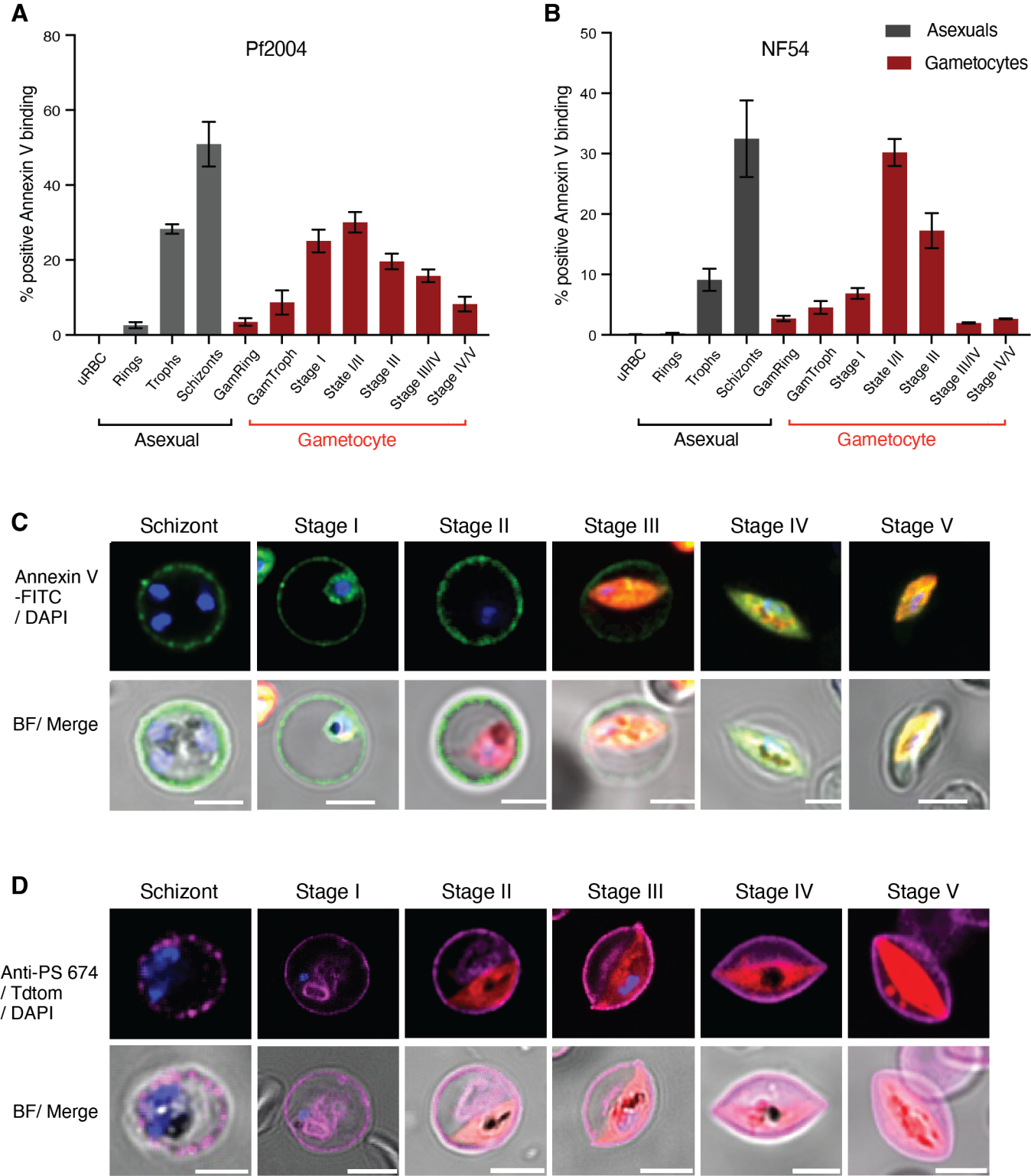
A
Pf2004
% positive Annexin V binding
80
60
40
20
0
uRBC
Rings
Trophs
Schizonts
GamRing
GamTroph
Stage I
State I/II
Stage III
Stage III/IV
Stage IV/V
Asexual
Gametocyte
B
NF54
Asexuals
Gametocytes
% positive Annexin V binding
50
40
30
20
10
0
uRBC
Rings
Trophs
Schizonts
GamRing
GamTroph
Stage I
State I/II
Stage III
Stage III/IV
Stage IV/V
Asexual
Gametocyte
C
Schizont
Stage I
Stage II
Stage III
Stage IV
Stage V
Annexin V
-FITC
/ DAPI
BF/ Merge
D
Schizont
Stage I
Stage II
Stage III
Stage IV
Stage V
Anti-PS 674
/ Tdtom
/ DAPI
BF/ Merge

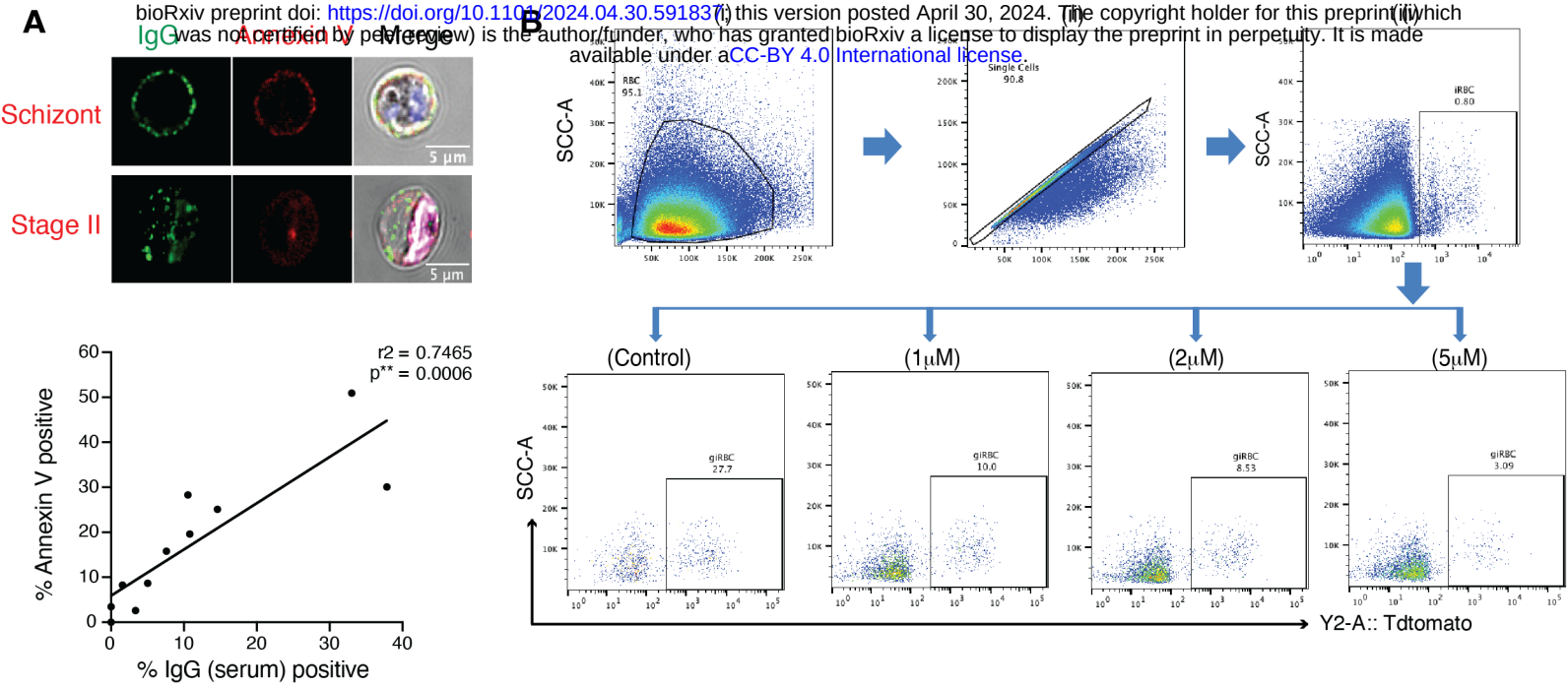

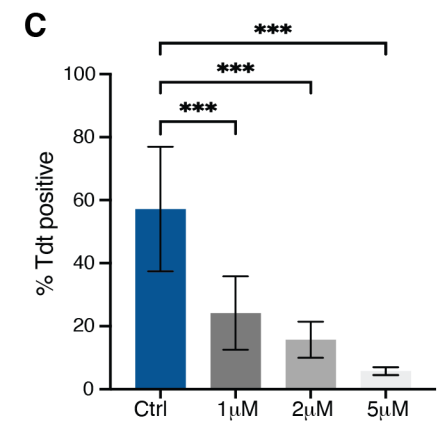

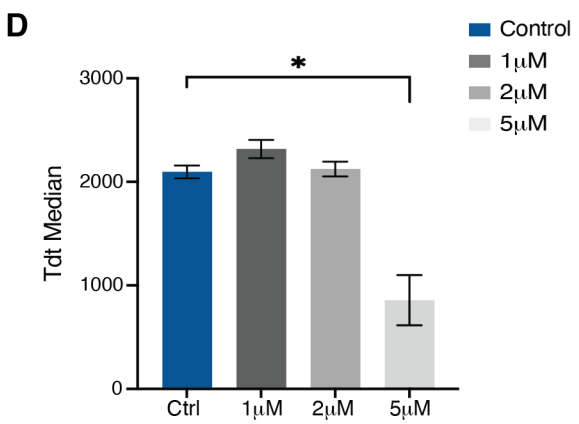

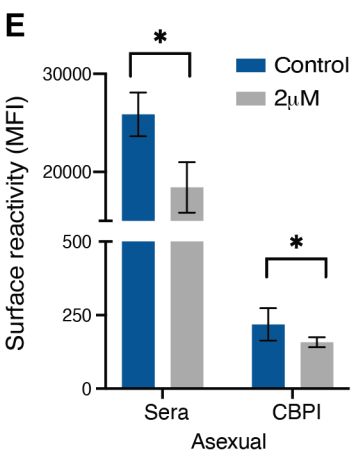

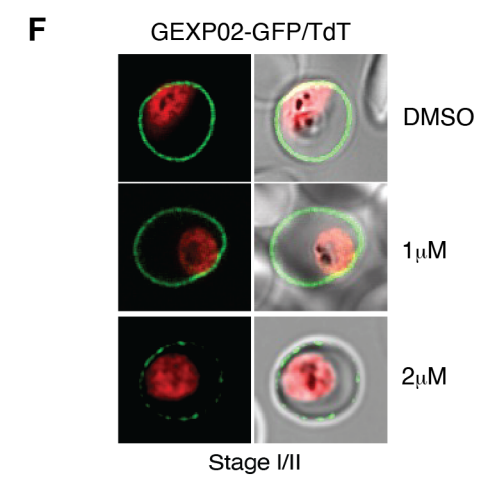

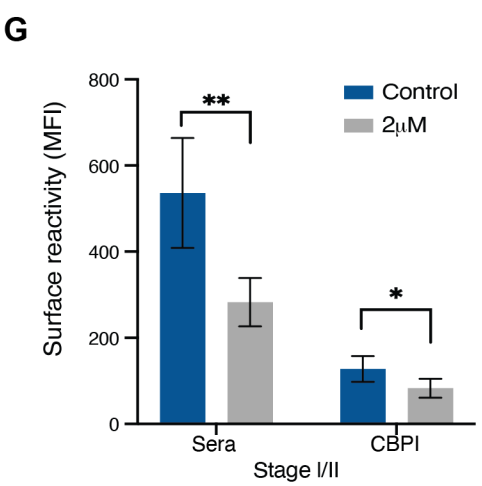

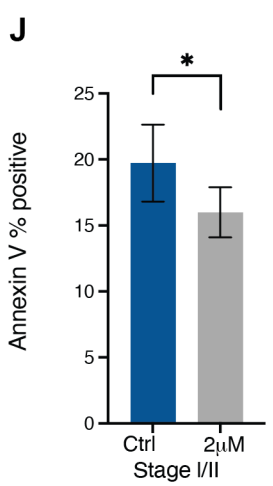

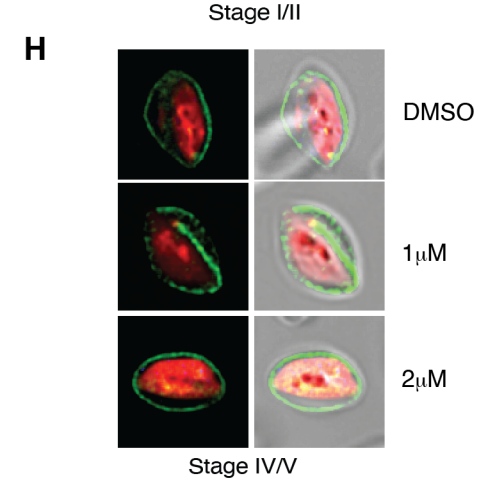

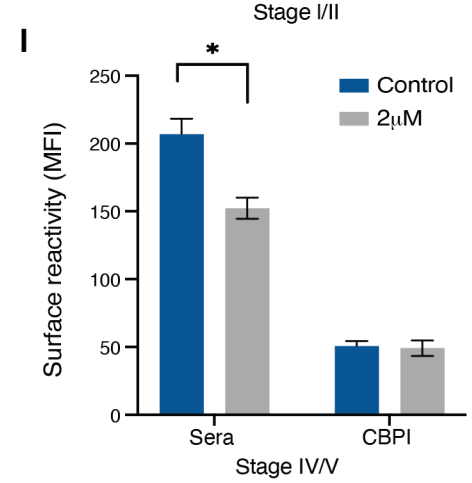

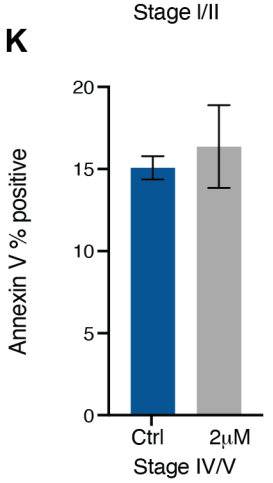

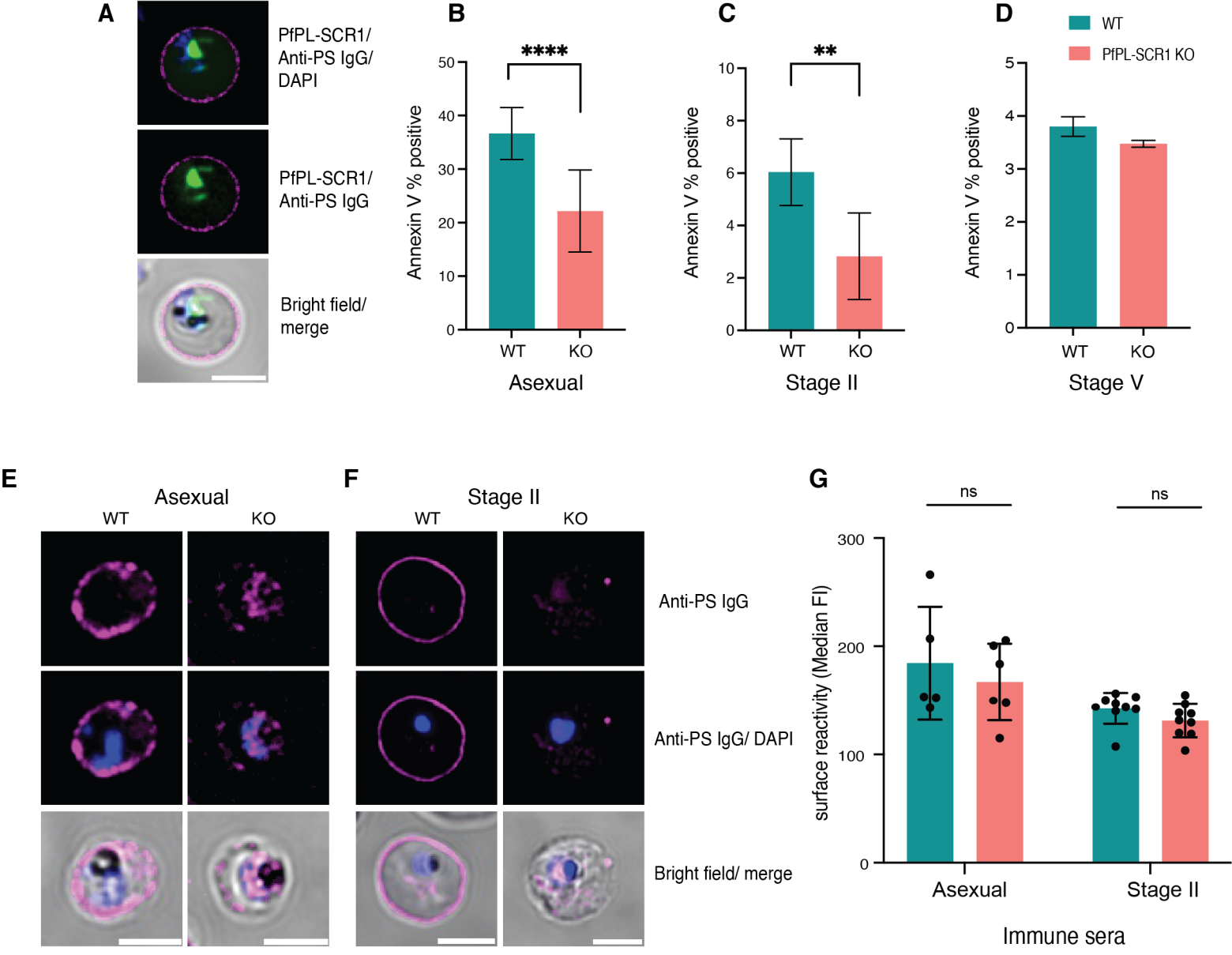
A
PfPL-SCR1/ Anti-PS IgG/ DAPI
PfPL-SCR1/ Anti-PS IgG
Bright field/ merge
B
****
Annexin V % positive
50
40
30
20
10
0
WT
KO
Asexual
C
**
Annexin V % positive
10
8
6
4
2
0
WT
KO
Stage II
D
WT
PfPL-SCR1 KO
Annexin V % positive
5
4
3
2
1
0
WT
KO
Stage V
E
Asexual
WT
KO
F
Stage II
WT
KO
Anti-PS IgG
Anti-PS IgG/ DAPI
Bright field/ merge
G
ns
ns
surface reactivity (Median FI)
300
200
100
0
Asexual
Stage II
Immune sera

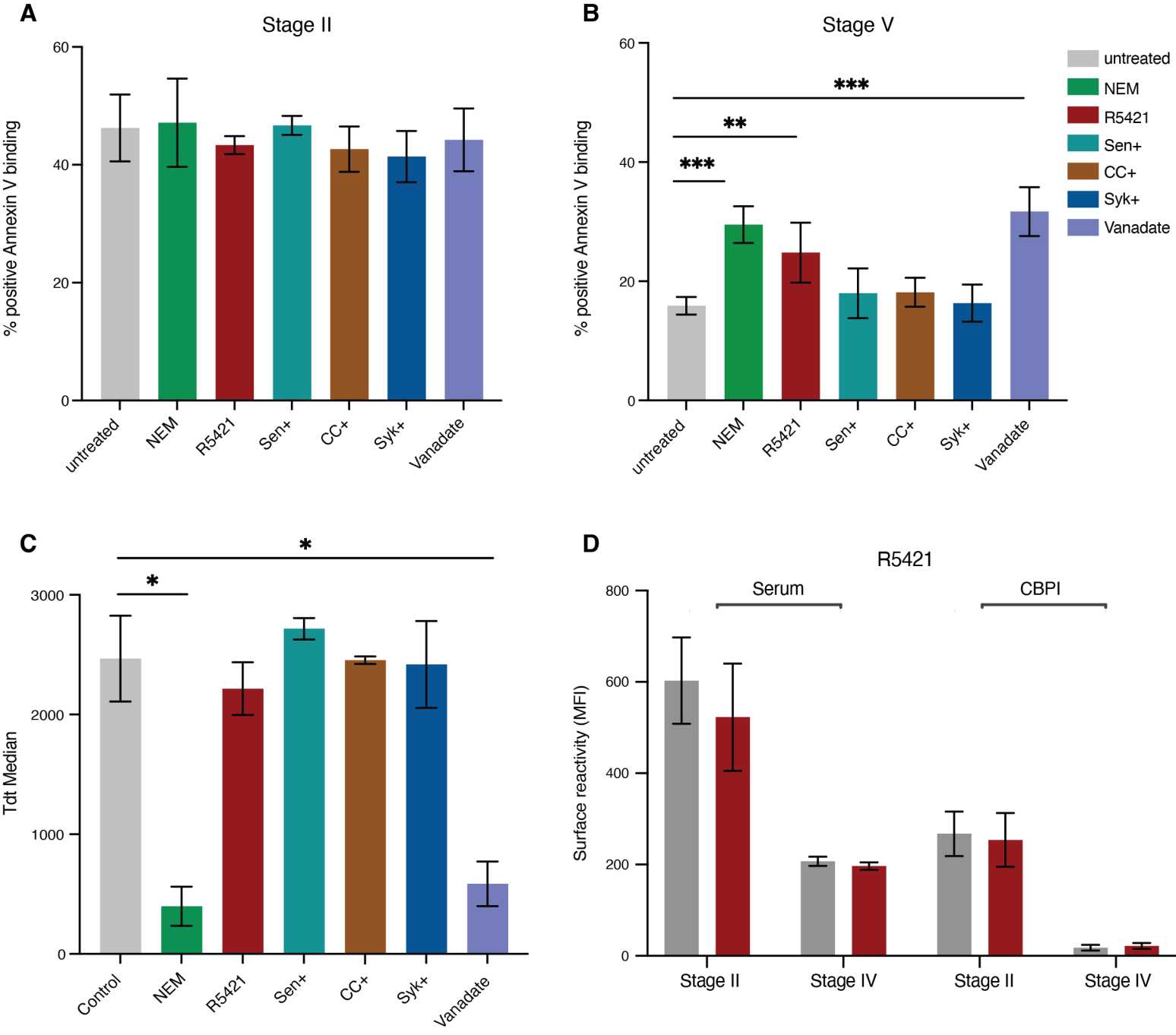
A
Stage II
% positive Annexin V binding
60
40
20
0
untreated
NEM
R5421
Sen+
CC+
Syk+
Vanadate
B
Stage V
% positive Annexin V binding
***
**
***
untreated
NEM
R5421
Sen+
CC+
Syk+
Vanadate
C
*
*
Tdt Median
3000
2000
1000
0
Control
NEM
R5421
Sen+
CC+
Syk+
Vanadate
D
R5421
Serum
CBPI
Surface reactivity (MFI)
800
600
400
200
0
Stage II
Stage IV
Stage II
Stage IV

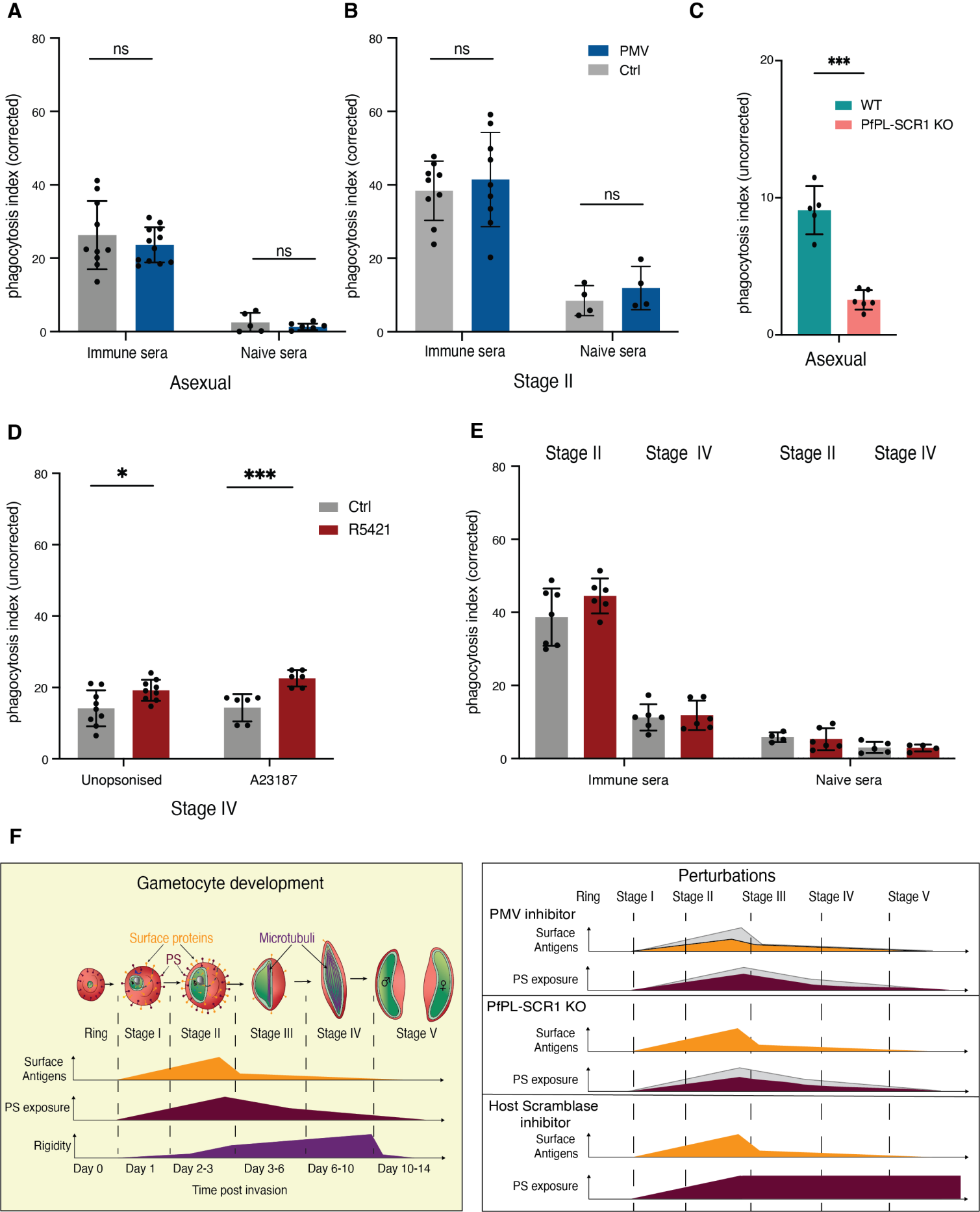
A
B
C
D
E
F
phagocytosis index (corrected)
phagocytosis index (uncorrected)
ns
*
***
PMV
Ctrl
WT
PfPL-SCR1 KO
R5421
Immune sera
Naive sera
Asexual
Stage II
Stage IV
Unopsonised
A23187
Gametocyte development
Surface proteins
PS
Microtubuli
Ring
Stage I
Stage II
Stage III
Stage IV
Stage V
Surface Antigens
PS exposure
Rigidity
Day 0
Day 1
Day 2-3
Day 3-6
Day 6-10
Day 10-14
Time post invasion
Perturbations
PMV inhibitor
PfPL-SCR1 KO
Host Scramblase inhibitor